Journal of Statistical Physics, Vol. 44, Nos. 3/4, 1986

Collapse Transition and Asymptotic Scaling Behavior of Lattice Animals: Low-Temperature Expansion

Ronald Dickman[1,2] and William C. Schieve[1]

Received December 17, 1985; final March 10, 1986

A low-temperature expansion for the free energy density of lattice animals is derived. Analysis of the series yields a collapse transition temperature of $T_c \simeq 0.54$, in close agreement with previous estimates. It is demonstrated that $\sigma_{p,k}$, the number of p-particle, k-bond animals, obeys the asymptotic scaling law $\log \sigma_{p,k} \sim p\tilde{g}(k/p) + o(p)$. The low-temperature series and numerical data are used to estimate the scaling function.

KEY WORDS: Lattice animals; collapse transition; low-temperature expansion.

1. INTRODUCTION

Lattice animals—collections of particles occupying the sites of a regular lattice and connected by a network of nearest-neighbor bonds—are of continuing interest in theories of nucleation[1-3] and percolation,[4,5] where they serve as a model of physical clusters. More recently, animals have been proposed as a model for branched polymers.[6-10] In particular, the collapse of a large branched polymer, as a function of polymer–solvent affinity, has been investigated by introducing a nearest-neighbor attractive potential between particles within the animal. At low temperatures (correspond to poor solvent), the animal is expected to assume a compact form, while at high temperatures a tenuous or ramified structure is favored entropically. Recent studies[6,7] indicate that in the infinite-size limit, animals undergo a second-order transition at the collapse temperature, T_c.

[1] Center for Studies in Statistical Mechanics, The University of Texas at Austin, Austin, Texas 78712.

[2] Present address: Dept. of Physics and Astronomy, Herbert H. Lehman College, C.U.N.Y., Bronx, New York 10468.

0022-4715/86/0800-0465$05.00/0

The statistics, thermal behavior, and geometry of lattice animals have been investigated via enumeration[10,11], renormalization group[8,12], phenomenological renormalization[6,13], and Monte Carlo[7,14–18] methods. In this paper we shall present new low-temperature expansion and numerical results bearing on the collapse transition of a single lattice animal, and on the asymptotic scaling behavior of the number of configurations of given size and degree of bonding.

Our earlier studies have focused on the p-particle animal partition function

$$Z_p(T) = \sum_{X \mid N(X) = p} e^{k(X)/T} = \sum_k \sigma_{p,k} e^{k/T} \tag{1.1}$$

The first sum is over translationally nonequivalent, connected configurations $X = \{x_1, ..., x_p\}$, where x_i lies in some lattice, e.g., $\mathbf{Z}^d$. $N(X)$ is the number of particles, $k(X)$ is the number of nearest-neighbor bonds, and T is the temperature, expressed in units such that $\varepsilon/k_B = 1$ (ε is the nearest-neighbor attractive potential, and k_B is Boltzmann's constant). In the second expression, $\sigma_{p,k}$ is the number of translationally nonequivalent, p-particle, k-bond connected configurations. We have employed enumeration and Monte Carlo methods to determine $\sigma_{p,k}$, and used the results to estimate scaling behavior[18] and to compute specific heats.[7] In this paper we derive a low-temperature expansion for the animal free energy density. To our knowledge, this is the first time that such an expansion has been derived for a system subject to a connectivity constraint.

In Sec. 2 we derive the low-temperature expansion for the free energy density, and discuss critical behavior. Some of the details of the derivation are given in Appendices A and B. In Sec. 3, numerical data for animals of up to 100 particles is used to test a previously proposed scaling law. The data is then reanalysed in light of the asymptotic scaling formula proven in Appendix C, yielding an estimate for the scaling function in the noncompact regime. Finally, in Sec. 4 the low-temperature series is used to derive an expansion for the asymptotic scaling function in the compact (low-temperature) regime. In this paper we consider the square lattice, $\mathbf{Z}^2$, only. Preliminary results for other lattices suggest similar quantitative behavior.

2. LOW-TEMPERATURE EXPANSION

2.1. Approximate Partition Function

In this section we derive a low-temperature expansion for the free energy density of animals in the square lattice. Since the animal partition function, Eq. (1.1), is not directly amenable to a systematic low-tem-

perature expansion, we first show how the free energy may, at low temperatures, be computed from an approximate partition function, which resembles the grand partition function for a lattice gas. Our derivation rests on the assumption that, at low temperatures, animals are *compact*. Define the *perimeter* of an animal as the minimal, simple closed path, residing in the dual lattice, which encloses all sites occupied by the animal, as depicted in Fig. 1. (Note that vacant sites within the animal are also enclosed.) Let $B(X)$ be the perimeter length of animal configuration X. ($B(X)$ is the number of lattice bonds which cut the perimeter.) We shall say that animals are compact at temperature T if, for some $b(T) < \infty$,

$$\kappa_a(T) \equiv \lim_{p \to \infty} p^{-1} \log Z_p(T) = \lim_{p \to \infty} p^{-1} \log \sum_{X | B(X) \leqslant b\sqrt{p}; N(X) = p} e^{k(X)/T} \quad (2.1)$$

i.e., if configurations with perimeter larger than $b\sqrt{p}$ make a negligible contribution to the free energy. The existence of the animal free energy density, $-T\kappa_a(T)$, was demonstrated in Ref. 21. Clearly, Eq. (2.1) holds for $T=0$ ($b(0)=4$), and we shall assume that it remains true for $0 < T < T_c$. There is strong numerical evidence,[6,7] although as yet no rigorous proof, that animals exhibit a collapse transition at a finite temperature, below which they are compact.

At low temperatures ($T < T_c$), a p-particle animal may be pictured as a compact region of p occupied and v vacant sites. (This picture must of course fail at T_c, for then $b(T) \to \infty$.) If all $p+v$ sites were occupied, there would be $2(p+v) - O(\sqrt{p})$ bonds. Each isolated vacancy represents a loss of four bonds, and each nearest-neighbor pair of vacancies yields a net gain

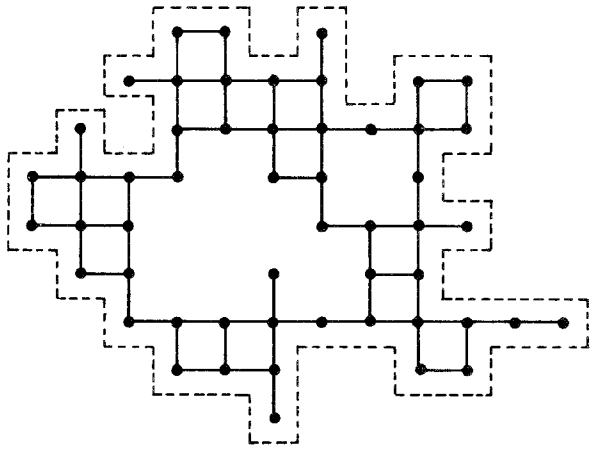

Fig. 1. A lattice animal and its perimeter (broken line).

of one bond over the situation in which the vacancies are separated by more than a unit distance. Vacancies at sites x_i and $x_j \in \mathbf{Z}^2$ therefore interact with an effective potential

$$u(|x_i - x_j|) = \begin{cases} +\infty, & x_i = x_j \\ -1, & |x_i - x_j| = 1 \\ 0, & \text{otherwise} \end{cases} \tag{2.2}$$

(We wish to exclude the possibility of two vacancies "occupying" the same site.) The energy of a compact ($B(X) \leqslant b(T)\sqrt{p}$) p-particle animal with vacancies at sites $x_1, ..., x_v$ within its perimeter is $-2(p-v) + U(x_1, ..., x_v) + O(\sqrt{p})$, where

$$U(x_1, ..., x_v) = \sum_{1 \leqslant i < j \leqslant v} u(|x_i - x_j|) \tag{2.3}$$

According to the compactness assumption, Eq. (2.1), we may, for purposes of computing the free energy density, restrict the partition function to configurations with perimeter $B \leqslant b(T)\sqrt{p}$. All such configurations fit inside a square of side $\frac{1}{2}b\sqrt{p}$. Thus if we define

$$Z_p''(T) = \sum_{X \subset \Lambda_{b^2(T)p/4} | N(X) = p} e^{k(X)/T} \tag{2.4}$$

where $\Lambda_N \subset \mathbf{Z}^2$ is the smallest square containing at least N sites, then we are assured that $\lim_{p \to \infty} p^{-1} \log Z_p''(T) = \kappa_a(T)$.

For $p = q^2$ ($q = 1, 2, 3, ...$), define the modified partition function

$$Z_p'(T) = \xi^{2p} \sum_{m=0}^{m_{\max}} \frac{\xi^{-2v}}{v!} \sum_{\bar{x}_1, ..., \bar{x}_v \in \Lambda_{p+v}}^{c} e^{-U(\bar{x}_1, ..., \bar{x}_v)/T} \tag{2.5}$$

where $\xi = e^{1/T}$, $v = m(2q + m)$ is the number of vacancies, and the second sum is over the positions of the vacancies within Λ_{p+v}, a square of $q + m$ sites on a side. The upper limit on m is $m_{\max} = [(b(T)/2 - 1)\sqrt{p} + 1]$ (largest integer), so that for $m = m_{\max}$, $\Lambda_{p+v} = \Lambda_{b^2p/4}$. The superscript "c" on the second sum denotes a connectivity constraint: only configurations in which the set of occupied sites, $\Lambda_{p+v} \backslash \{\bar{x}_1, ..., \bar{x}_v\}$, is connected by a network of nearest-neigbor bonds are permitted.

There is a many-to-one correspondence between vacancy configurations $\bar{X} = \{\bar{x}_1, ..., \bar{x}_v\}$ in Z_p', and the particle configurations $X = \{x_1, ..., x_p\}$ in Z_p'', where $X = \Lambda_{p+v} \backslash \bar{X}$. (More precisely, the correspondence is between $\bar{X}$ and an *equivalence class* of X's differing solely by a uniform translation. Each equivalence class occurs exactly once in Z_p''.) In Z_p', $\bar{X}$ is

assigned energy $-2(p-v)+U(\bar{X})$. The correct energy, assigned to $X=\Lambda_{p+v}\backslash\bar{X}$ in Z''_p, is shown in Appendix A to be

$$-k(X)=-\{2(p-v_{\text{in}})-\tfrac{1}{2}B(X)\}+U_{\text{in}} \tag{2.6}$$

where v_{in} is the number of vacancies enclosed by the perimeter of X, and $-U_{\text{in}}$ is the number of nearest-neighbor bonds between such vacancies. As is shown in Appendix A, the difference between $-2(p-v)+U(\bar{X})$ and the true energy is

$$\Delta E=v_{\text{e}}+2v_{\text{c}}-2(\sqrt{p}+m) \tag{2.7}$$

where v_{e} and v_{c} are respectively, the number of vacancies lying at edges and at corners of Λ_{p+v}. It follows that $|\Delta E|\leqslant 2b(T)\sqrt{p}$.

For each X occuring in Z''_p there is at least one corresponding $\bar{X}$ in Z'_p. But since configurations which fit inside Λ_{p+v} also fit inside larger squares, and since vacancy configurations which differ by a uniform translation within Λ_{p+v} are counted as distinct in Z'_p, there are, in general, several $\bar{X}$'s corresponding to a given X. For any of the $(b/2-1)\sqrt{p}+1$ possible m values in Z'_p, there are fewer than $p+v(m)$ translationally equivalent $\bar{X}$'s corresponding to a given X in Z''_p. Thus

$$e^{-2b(T)\sqrt{p}}Z''_p(T)\leqslant Z'_p(T)$$

$$<\frac{b^2(T)}{4}\left[(\tfrac{1}{2}b(T)-1)\sqrt{p}+1\right]e^{2b(T)\sqrt{p}}Z''_p(T) \tag{2.8}$$

which implies that for $b(T)<\infty$ (i.e., $T<T_{\text{c}}$),

$$\lim_{p\to\infty}p^{-1}\log Z'_p(T)=\kappa_{\text{a}}(T) \tag{2.9}$$

2.2. Free Energy Density

We shall use Z'_p as a basis for deriving a low-temperature expansion for $\kappa_{\text{a}}(T)$. Z'_p resembles the grand partition function of a lattice gas in that it is a sum over the number and positions of vacancies, with nearest-neighbor interaction U. Expansion of the free energy density in powers of $e^{-1/T}$ is, however, still not straightforward, because of the restriction to connected configurations, and the fact that Z'_p is not defined with respect to a fixed volume. Instead of attempting to apply graph expansion methods

directly to Z'_p, we shall relate $\kappa_a(T)$ to a free energy density for connected configurations in a fixed-volume ensemble. The latter may be evaluated by considering a lattice gas with many-body interactions. We begin by noting that the grand partition function for a lattice gas of N sites (periodic boundary conditions), with nearest-neighbor, attractive interactions may be written in the form

$$\Xi(N, T, \mu) = \xi^{2N}\lambda^{-N} \sum_{n=0}^{1} \frac{\xi^{-4Nn}\lambda^{Nn}}{(Nn)!} \sum_{x_1,\ldots,x_{Nn} \in \Lambda_N} e^{-U(x_1,\ldots,x_{Nn})/T} \tag{2.10}$$

where $\lambda = e^{-\mu/T}$, and μ is the chemical potential. Nn, the number of vacancies, takes the values 0, 1,..., N. We shall denote by $\Xi^c(N, T, \mu)$ the r.h.s. of Eq. (2.10) with the second sum restricted to connected configurations, as in Z'_p. Define the free energy density associated with vacancy density n (n rational) by

$$z(T, n) \equiv \lim_{N\to\infty} N^{-1} \log \left\{ [(Nn)!]^{-1} \sum_{x_1,\ldots,x_{Nn} \in \Lambda_N} e^{-U(x_1,\ldots,x_{Nn})/T} \right\} \tag{2.11}$$

where $N \to \infty$ through integers $N = q^2$ such that Nn is an integer. Let the r.h.s. of Eq. (2.11) with the sum restricted to connected configurations define $z^c(T, n)$. From Eqs. (2.10) and (2.11) we have

$$\begin{aligned} \kappa(T, \mu) &\equiv \lim_{N\to\infty} N^{-1} \log \Xi(N, T, \mu) \\ &= \sup_{0\le n\le 1} \left[\frac{2-4n}{T} + \frac{(1-n)\,\mu}{T} + z(T, n) \right] \\ &= \frac{2-4\bar{n}(T,\mu)}{T} + \frac{[1-\bar{n}(T,\mu)]\,\mu}{T} + z(T, \bar{n}(T,\mu)) \end{aligned} \tag{2.12}$$

A similar relation holds between $\kappa_c(T, \mu) \equiv \lim_{N\to\infty} N^{-1} \log \Xi^c(N, T, \mu)$ and $z^c(T, n)$, with the location of the maximum defining $\bar{n}_c(T, \mu)$.

As $p \to \infty$, the values taken on by $n' = v/p$ in Z'_p, Eq. (2.5), become dense in the interval $[0, b^2(T)/4 - 1]$, and we may write

$$\begin{aligned} \lim_{p\to\infty} p^{-1} \log Z'_p = \frac{2}{T} + \lim_{p\to\infty} p^{-1} \sup_{n'\ge 0} \log \Bigg\{ &\xi^{-2n'p} [(n'p)!]^{-1} \\ &\times \sum_{x_1,\ldots,x_{n'p} \in \Lambda_{p(1+n')}}^{c} e^{-U(x_1,\ldots,x_{n'p})/T} \Bigg\} \end{aligned} \tag{2.13}$$

Let $N=(1+n')p$ and $n=n'/(1+n')$. Then Eq. (2.13) becomes

$$\lim_{p\to\infty} p^{-1}\log Z'_p=\frac{2}{T}+\sup_{n\geqslant 0}\lim_{N\to\infty}[N(1-n)]^{-1}\log\left\{\xi^{-2Nn}[(Nn)!]^{-1}\times\sum_{x_1,\ldots,x_{Nn}\in\Lambda_N}{}^{c} e^{-U(x_1,\ldots,x_{Nn})/T}\right\}$$

$$=\frac{2}{T}+\sup_{n\geqslant 0}\frac{z^c(T,n)-2n}{1-n}$$

$$=\frac{2}{T}+\frac{z^c(T,\bar{n}_a(T))-2\bar{n}_a(T)}{1-\bar{n}_a(T)} \tag{2.14}$$

$\bar{n}_a(T)$ is the limiting average vacancy density (per *site*) in animals. To determine $\kappa_a(T)$ and $\bar{n}_a(T)$ we require $z^c(T,n)$, which may in turn be found once $\kappa_c(T,\mu)$ and $\bar{n}_c(T,\mu)$ are known.

The low-temperature expansion for $\kappa_c(T,\mu)$ may be obtained by adding certain connectivity corrections to the expansion for $\kappa(T,\mu)$. The latter is known from series expansions for the Ising model. If $Z_I(N,T,h)$ is the partition function for a nearest-neighbor, ferromagnetic Ising lattice of N sites (periodic boundary conditions), at temperature T and external field h, then we have the well-known relation

$$\Xi(N,T,\mu)=(\xi/\lambda)^{N/2}Z_I(N,4T,2\mu+4) \tag{2.15}$$

which implies

$$\kappa(T,\mu)=\frac{1+\mu}{2T}+\lim_{N\to\infty}N^{-1}\log Z_I(N,4T,2\mu+4)$$

$$=\frac{1+\mu}{2T}+\kappa_I(4T,2\mu+4) \tag{2.16}$$

Using results for $\kappa_I(T,h)$ derived by Sykes *et al.*,[19] one finds that

$$\kappa(T,\mu)=\frac{2+\mu}{T}+\sum_{r=1}^{\infty}\lambda^r\eta^{2r}g_r(\eta) \tag{2.17}$$

where $\eta=\xi^{-1}=e^{-1/T}$. The polynomials g_r are tabulated for $r\leqslant 15$ (square lattice) in Ref. 20, and, using the graph expansion methods described in that review, one readily finds that $g_{16}=\eta^8+O(\eta^9)$, and that g_r is of order η^9 or higher for $r>16$. We shall compute κ_a to order η^8, and so the sum in

Eq. (2.17) may be truncated at $r=16$. On the phase coexistence line, $\lambda\eta^2=1$, Eq. (2.17) becomes[19]

$$\kappa_{\text{coex}}(T)=\eta^2+2\eta^3+\tfrac{9}{2}\eta^4+12\eta^5+37\tfrac{1}{3}\eta^6+130\eta^7+490\tfrac{1}{4}\eta^8+\cdots \quad (2.18)$$

The vacancy density in the lattice gas is

$$\bar{n}(T,\mu)=\lambda\frac{\partial}{\partial\lambda}\kappa(T,\mu)+\lambda=\sum_{r=1}^{\infty} r\lambda^r\eta^{2r}g_r(\eta) \quad (2.19)$$

and on the coexistence line[19]

$$\bar{n}_{\text{coex}}(T)=\eta^2+4\eta^3+17\eta^4+76\eta^5+357\eta^6+\cdots \quad (2.20)$$

We turn now to the evaluation of $\kappa_c(T,\mu)$. In Ξ^c only connected configurations are allowed, and this proves inconvenient from the graph expansion viewpoint. To circumvent this difficulty, we introduce many-body interactions into the vacancy potential U, so as to exclude disconnected configurations. Then Ξ^c may be expressed as an unrestricted sum over the modified potential, and a low temperature expansion for κ_c may be derived via the Ursell expansion. Define the potential $U_c(\bar{X})$ ($\bar{X}=\{\bar{x}_1,\ldots,\bar{x}_n\}\subset\Lambda_N$) such that $U_c(\bar{X})=U(\bar{X})$ if the set of occupied sites $\Lambda_N\backslash\bar{X}$ is connected, and $U_c(\bar{X})=+\infty$ otherwise. Replacing U by U_c in the r.h.s.

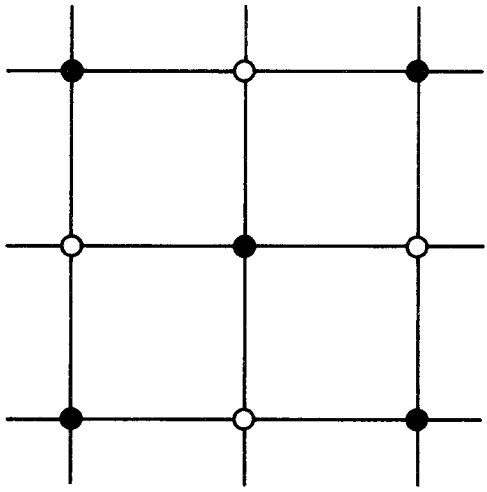

Fig. 2. Arrangement of four vacancies (open circles) surrounding a particle (filled circles), which is excluded by U_c.

of Eq. (2.10) yields $\Xi^c(N, T, \mu)$. We shall impose the connectivity constraint through the condition: no set of occupied sites may be encircled by vacacies. When the vacancy density is low (as it is at low temperatures: $\bar{n} \sim e^{-2/T}$), this restriction on the configurations of vacancies within a "sea" of occupied sites effectively eliminates disconnected configurations, since the vacancies cannot percolate on Λ_N for large N. The lowest-order term in $U_c - U$ involves four vacancies, and assigns energy $+\infty$ to the configuration shown in Fig. 2. Subsequent terms serve to prohibit six vacancies from encircling a pair of occupied sites, and so on.

As is shown in Appendix B, application of the Ursell expansion[22] leads to

$$\kappa_c(T, \mu) = \frac{2+\mu}{T} + \sum_{r=1}^{\infty} \lambda^r \eta^{2r} g_r^c(\eta) \tag{2.21}$$

where

$$\begin{aligned}
g_r^c &= g_r, \qquad r \leqslant 3 \\
g_4^c &= g_4 - \eta^8 \\
g_5^c &= g_5 - 4\eta^8 - 4\eta^9 + 17\eta^{10} \\
g_6^c &= g_6 - 6\eta^8 - 24\eta^9 + O(\eta^{10}) \\
g_7^c &= g_7 - 4\eta^8 - 56\eta^9 + O(\eta^{10}) \\
g_8^c &= g_8 - \eta^8 - 64\eta^9 + O(\eta^{10}) \\
g_r^c &= g_r + O(\eta^9), \qquad r \geqslant 9
\end{aligned} \tag{2.22}$$

Using these results, we may derive an expansion for $z^c(T, n)$. From Eq. (2.12) we have

$$\left.\frac{\partial z^c(T, n)}{\partial n}\right|_{n = \bar{n}_c(T,\mu)} = \frac{4+\mu}{T} \tag{2.23}$$

Into this relation we insert the expansion

$$z^c(T, n) = -n \log n + \sum_{r=1}^{\infty} n^r h_r^c(\xi) \tag{2.24}$$

as well as

$$\bar{n}_c(T, \mu) = \sum_{r=1}^{\infty} r \lambda^r \eta^{2r} g_r^c(\eta) \tag{2.25}$$

(Note that, in light of Eq. (2.22), $\bar{n}_{c,coex} = \bar{n}_{coex} + O(\eta^8)$.) Upon equating coefficients of powers of λ we find

$$\begin{aligned}
h_1^c &= 1 \\
h_2^c &= 2\xi - \tfrac{5}{2} \\
h_3^c &= -2\xi^2 + 4\xi - \tfrac{13}{6} \\
h_4^c &= \xi^4 - \tfrac{2}{3}\xi^3 - 3\xi^2 + 4\xi - \tfrac{29}{12} \\
h_5^c &= -8\xi^5 + 29\xi^4 + O(\xi^3) \\
h_6^c &= 2\xi^7 + 32\xi^6 + O(\xi^5) \\
h_7^c &= -34\xi^8 + O(\xi^7) \\
h_8^c &= 6\xi^{10} + O(\xi^9) \\
h_9^c &= \xi^{12} + O(\xi^{11})
\end{aligned} \tag{2.26}$$

From Eq. (2.14) we have

$$\frac{\partial}{\partial n}\left\{(1-n)^{-1}\left[z^c(T,n) - \frac{2n}{T}\right]\right\}_{n=\bar{n}_a} = 0 \tag{2.27}$$

Inserting the expansion $\bar{n}_a = a_2\eta^2 + a_3\eta^3 + \cdots$, and our result for $z^c(T, n)$, one finds, on equating coefficients of powers of η,

$$\bar{n}_a(T) = \eta^2 + 4\eta^3 + 18\eta^4 + 86\eta^5 + 439\eta^6 + \cdots \tag{2.28}$$

Note that

$$\begin{aligned}
z^c(T,\bar{n}_a) - \frac{2\bar{n}_a}{T} &= z^c(T,\bar{n}_{c,coex}) - \frac{2\bar{n}_{c,coex}}{T} \\
&= \frac{1}{2}\frac{\partial^2 z^c(T,n)}{\partial n^2}\bigg|_{n=\bar{n}_{c,coex}} (\bar{n}_a - \bar{n}_{c,coex})^2 \\
&\quad + \frac{1}{6}\frac{\partial^3 z^c(T,n)}{\partial n^3}\bigg|_{n=\bar{n}_{c,coex}} (\bar{n}_a - \bar{n}_{c,coex})^3 + O(\eta^9) \\
&= \kappa_{c,coex} - \frac{1}{2}\eta^6 - 6\eta^7 - 53\frac{5}{6}\eta^8 + O(\eta^9)
\end{aligned} \tag{2.29}$$

where we used Eq. (2.12) and our results for z^c, $\bar{n}_c$, and $\bar{n}_a$. Using Eqs. (2.28) and (2.29) in (2.14), we finally obtain

$$\kappa_a(T) = \frac{2}{T} + \sum_{r=2}^{\infty} c_r \eta^r$$
$$= \frac{2}{T} + \eta^2 + 2\eta^3 + \frac{11}{2}\eta^4 + 18\eta^5 + 68\frac{1}{3}\eta^3 + 286\eta^7 + 1270\frac{3}{4}\eta^8 + \cdots \tag{2.30}$$

which is the desired low-temperature expansion for the animal free energy density.

A simple approximation for the animal free energy density at low temperatures is

$$\kappa_a(T) - \frac{2}{T} = \frac{\kappa_{coex}(T)}{1 - \bar{n}_{coex}(T)} \tag{2.31}$$

Such an approximation was employed by Jaccuci *et al.*[17] in comparing Monte Carlo calculations of cluster (animal) free energies with the predictions of a modified droplet model. Equation (2.31) effectively treats animals as if they were subject to a finite pressure (the coexistence pressure in the lattice gas), whereas, by definition, animals exist at zero pressure. Moreover, the above approximation ignores the connectivity constraint. Nonetheless, Eq. (2.31) is an excellent approximation at low temperatures. Inserting Eqs. (2.18) and (2.20), we find that

$$\frac{\kappa_{coex}(T)}{1 - \bar{n}_{coex}(T)} = \eta^2 + 2\eta^3 + \frac{11}{2}\eta^4 + 18\eta^5 + 67\frac{5}{6}\eta^6 + 280\eta^7 + 1232\frac{7}{12}\eta^8 + \cdots$$
$$= \kappa_a(T) - \frac{2}{T} - \frac{1}{2}\eta^6 - 6\eta^7 - 38\frac{1}{6}\eta^8 + \cdots \tag{2.32}$$

Even for $T = 0.5$ ($T/T_c \simeq 0.93$), the two expressions for $\kappa_a - 2/T$ differ by less than 0.05%.

2.3. Collapse Transition

One expects the animal free energy density, κ_a to be singular at T_c, the collapse transition temperature. Thus the radius of convergence of the low-temperature expansion, Eq. (2.30), should be given by $\eta_c = e^{-1/T_c}$. We estimate the radius of convergence by examining the ratios, $v_n = c_n/c_{n-1}$, of successive coefficients in the series (see Fig. 3). The last four ratios fall close to a line of the form

$$v_n = v\left(1 - \frac{b}{n}\right) \tag{2.33}$$

In Table I we list the estimates for v, $T_c = (\log v)^{-1}$, and b, obtained by extending line segments connecting successive pairs of points to the $n = \infty$

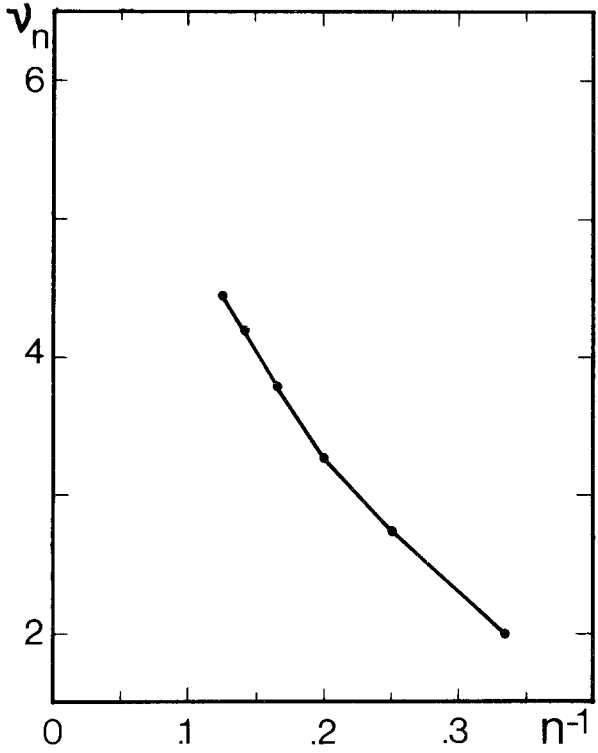

Fig. 3. Ratios, ν_n, of successive coefficients in the low-temperature expansion of the animal free energy density, Eq. (2.30), versus $1/n$.

Table I. Estimates of Critical Parameters Based on Ratios of Successive Coefficients in Eq. (2.30)

Interval	ν	T_c	b
4–5	5.3636	0.595	1.9492
5–6	6.4141	0.538	2.4488
6–7	6.5198	0.533	2.5064
7–8	6.2479	0.546	2.3073

axis. The average of the last three estimates yields $T_c \simeq 0.54$. Due to the shortness of the series, it is difficult to judge the uncertainty of this estimate. As η approaches η_c from below, the singular part of the animal free energy density scales as $\kappa_{a,\text{sing}} \propto (1-\eta/\eta_c)^{b-1}$. The specific heat per particle is

$$c_a(T) = T^{-2}\left[\frac{\partial \kappa_a}{\partial \eta} + \eta \frac{\partial^2 \kappa_a}{\partial \eta^2}\right] \tag{2.34}$$

and so the specific heat critical exponent is $\alpha = 3 - b$. The last three intervals in Table I yield the estimate: $\alpha \simeq 0.58$.

A phenomenological renormalization study by Derrida and Herrmann[6] furnished the estimates: $T_c = 0.535 \pm 0.005$, and $\alpha \simeq 0.48$. A Monte Carlo study by the present authors[7] generated specific heat data (for animals of 100 or fewer particles) which was consistent with the Derrida–Herrmann estimate for T_c. Thus the collapse temperature of square lattice animals has been estimated by three independent methods, and the results are mutually consistent. Owing to the shortness of the presently available series, the expansions for the animal specific heat and vacancy density do not yield useful results regarding critical behavior, when analyzed using either ratio or Pade approximant methods.

In Ref. 7 it was remarked that the collapse temperatures of both square and triangle lattice animals ($T_c \simeq 0.54$ and 0.90, respectively) are close to the critical temperatures ($T_{cr} \simeq 0.567$ and 0.912, respectively) of the corresponding lattice gases. This is not surprising, given the close relation between the low-temperature expansions for the free energies of animals, and of the lattice gas on the coexistence line, revealed in our analysis. Animal collapse and the lattice gas critical point are, of course, qualitatively different transitions, characterized by different critical exponent values.

3. NUMERICAL TEST OF SCALING

In Ref. 18 we proposed and presented preliminary numerical evidence for a scaling formula for $\sigma_{p,k}$:

$$\log \sigma_{p,k} \sim \sigma_0(p) f[x(p,k)] \tag{3.1}$$

where

$$\sigma_0(p) = \sigma p - \theta \log p + c \tag{3.2}$$

with $\sigma \equiv \lim_{p\to\infty} p^{-1} \log \sum_k \sigma_{p,k}$, and, for square animals

$$x = \frac{k-p+1}{p-2\sqrt{p}+1} \tag{3.3}$$

So defined, x takes values in $[0, 1]$ as k varies between $p-1$ and $k_m(p) = [2(p-\sqrt{p})]$, the maximum possible number of bonds for a square animal of p particles. The term $\propto \sqrt{p}$ in the denominator of Eq. (3.3) reflects the surface bond deficit: Eq. (3.1) represents an attempt to describe both bulk and surface effects by means of a single scaling function.

Using Monte Carlo and enumeration methods described in Refs. 7 and 18, we have generated accurate estimates for $\sigma_{p,k}$ for square animals of up to 100 particles. To test the scaling hypothesis, we plot

$$f_p(x) \equiv \frac{\log \sigma_{p,k}}{\sup_k \log \sigma_{p,k}} \tag{3.4}$$

versus x in Fig. 4. The data for $p \geqslant 36$ is presented here for the first time; our earlier study of scaling[18] included data for $p \leqslant 32$ only. An

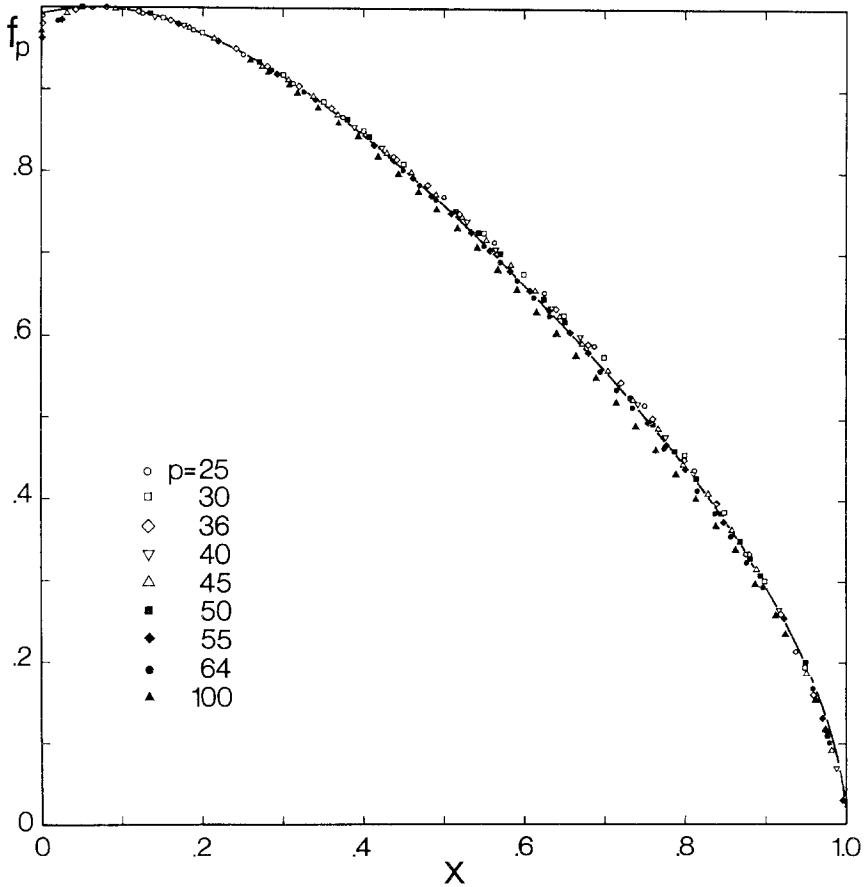

Fig. 4. $f_p(x)$, Eq.(3.4), versus x, Eq. (3.3), for square-lattice animals.

approximate scaling of the data is evident from the plot. Of interest is the accuracy with which the data may be fit by a simple, phenomenological scaling function. The solid line in Fig. 4 is of the form

$$f(x) = A(1-x)^{\gamma}[1 - a(x-z)^2 + b(x-z)^3] \tag{3.5}$$

The parameters were adjusted via a least-squares procedure, yielding, for the $p = 55$ data, the values $\gamma = 0.6$, $a = 0$, $b = 0.73$, and $z = 0.58$. (The prefactor A is fixed by the condition that f attain a maximum value of 1.) For $10 \leqslant p \leqslant 100$, the free energies calculated from Eqs. (3.1)–(3.3), with f given by Eq. (3.5), agree to within 1% with the Monte Carlo estimates. However, we do not believe that Eq. (3.5) is the correct asymptotic scaling function.

Despite the approximate scaling behavior, the $f_p(x)$ data do not appear to converge to an asymptotic scaling function. This is particularly striking when a comparison of the $p = 64$ and $p = 100$ data points is made. Now, if the scaling formula, Eq. (3.1), correctly described surface effects, we would expect $f_p(x)$ to converge to a limiting function, $f(x)$, such that $|f_p(x) - f(x)| \propto p^{-\zeta}$, with $\zeta > 1/2$. [That is, the corrections to Eq. (3.1) should be $o\sqrt{p}$).] However, a plot of $f_p(x)$ (for a given, fixed x), versus $p^{1/2}$ reveals no clear trend. Analysis of the data in accordance with Eqs. (3.3) and (3.4) does not permit estimation of the asymptotic scaling function.

In light of these observations, we believe that it is not possible to devise a scaling formula which incorporates surface as well as bulk effects in a single function. We shall focus instead on the bulk scaling behavior. In Appendix C we prove the asymptotic scaling formula

$$\log \sigma_{p,k} \sim p\tilde{g}\left(\frac{k}{p}\right) + o(p) \qquad (p \to \infty) \tag{3.6}$$

where $\tilde{g}$ is concave (hence continuous) on the rationals in $[1, q/2)$; (q is the coordination number of the lattice). The numerical data may be used to estimate the bulk scaling function as follows. Define a new scaling variable

$$y = \frac{k - p + 1}{p} \tag{3.7}$$

and let

$$g_p(y) \equiv \frac{\log \sigma_{p,k}}{\sup_k \log \sigma_{p,k}} \tag{3.8}$$

For convenience, the scaling variable y has been chosen to lie in $[0, 1]$, with trees ($k = p - 1$) always corresponding to $y = 0$. Since $y \to k/p - 1$

when $p \to \infty$, we expect $g_p(y) \to g(y) \equiv \sigma^{-1}\tilde{g}(y+1)$ when $p \to \infty$. The data for $\sigma_{p,k}$ furnish $g_p(y)$ for $y = 0,\ 1/p,\ldots,\ (k_m(p) - p + 1)/p$. We extend the definition of g_p to intermediate y values via linear interpolation. In Fig. 5 $g_p(y)$ is plotted versus p^{-1} for various values of y. For $y \leqslant 0.65$, the points converge rapidly to a straight line, whose intercept with the $p = \infty$ axis furnishes an estimate for the asymptotic scaling function, $g(y)$. For larger y values there is not sufficient data to permit accurate extrapolation. Our numerical estimate for $g(y)$ will be discussed in the following section.

A consequence of the scaling formula, Eq. (3.6), is that asymptotically, the number of animals $A_{p,c}$ with p particles and *cyclomatic index* c (the number of independent, closed paths through nearest neighbor bonds) grows at an exponential rate which is independent of c. Since animals are

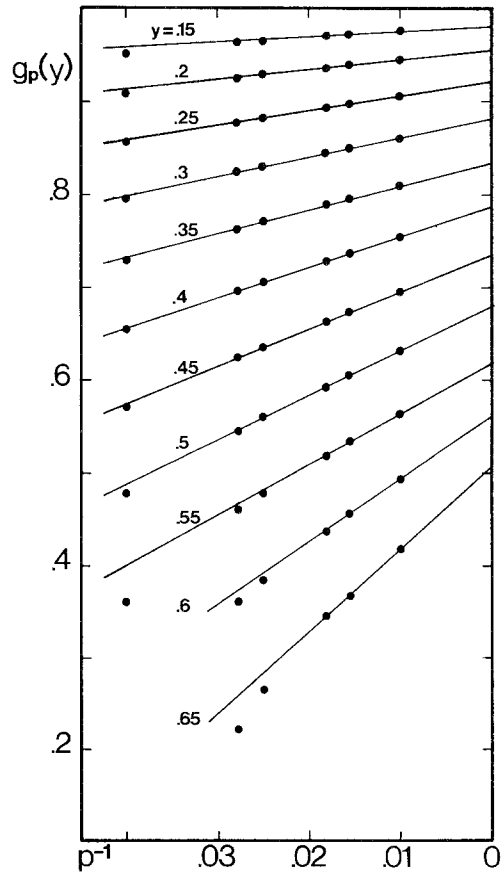

Fig. 5. $g_p(y)$, Eq. (3.8), versus $1/p$.

connected, Euler's theorem implies that a p-particle, k-bond animal has cyclomatic index $c = k - p + 1$. Thus $A_{p,c} = \sigma_{p,p+c-1}$, and from Eq. (3.6)

$$p^{-1} \log A_{p,c} \sim \tilde{g}\left(\frac{p+c-1}{p}\right) + o(1) \xrightarrow[p \to \infty]{} \tilde{g}(1) \equiv \sigma g(0) \tag{3.9}$$

which shows that the asymptotic rate of growth is indeed independent of c. Whittington *et al.*[10] proved the corresponding result for the rate of growth of the number of weak embeddings.

4. ASYMPTOTIC SCALING FUNCTION

In the preceding section we used numerical data for $\sigma_{p,k}$ to estimate the asymptotic scaling function, $g(y)$. Using the low-temperature expansion for the animal free energy density derived in Sec. 2, we may derive an expansion for $g(y)$ in the neighborhood of $y = 1$. Note that from Eqs. (3.6) and (3.7)

$$\begin{aligned} \kappa_a(T) &= \lim_{p \to \infty} p^{-1} \log \int_0^1 dy \exp\left[p\left(\frac{y+1}{T} + \sigma g(y)\right)\right] \\ &= -\frac{\bar{\varepsilon}(T)}{T} + \sigma g[-\bar{\varepsilon}(T) - 1] \end{aligned} \tag{4.1}$$

where $\bar{\varepsilon}(T)$ is the average energy per particle. From Eq. (2.30) we have

$$\begin{aligned} \bar{\varepsilon}(T) &= -\frac{d\kappa_a(T)}{d(1/T)} \\ &= -2 + 2\eta^2 + 6\eta^3 + 22\eta^4 + 90\eta^5 + 410\eta^6 + 2002\eta^7 + 10166\eta^8 + \cdots \end{aligned} \tag{4.2}$$

Combining Eqs. (4.1) and (2.30), we have

$$\sigma g(-\varepsilon - 1) = \frac{\bar{\varepsilon}}{T} + \frac{2}{T} + \eta^2 + 2\eta^3 + \cdots \tag{4.3}$$

Now since $1 + \bar{\varepsilon}/2 = \eta^2 + 3\eta^3 + \cdots$, it follows that

$$-\left(1 + \frac{\bar{\varepsilon}}{2}\right) \log\left(1 + \frac{\bar{\varepsilon}}{2}\right) = \frac{\bar{\varepsilon}}{T} + \frac{2}{T} + O(\eta^3) \tag{4.4}$$

which suggests that g has the form

$$\sigma g(-\varepsilon - 1) = -u \log u + a_1 u + a_{3/2} u^{3/2} + a_2 u^2 + \cdots \tag{4.5}$$

where $u = 1 + \varepsilon/2 = (1 - y)/2$. Half-integer powers of u are included in Eq. (4.5) because $(1 + \bar{\varepsilon}/2)^{n/2} = \eta^n + O(\eta^{n+1}) + \cdots$, while Eq. (4.3) is an expansion in powers of η. There is no term $\sim u^{1/2}$ since the right-hand side of Eq. (4.3) has no term $\sim \eta$. Substituting the above expansion into Eq. (4.3) and equating coefficients of η yields

$$\sigma g(y) = -u \log u + u + 2u^{3/2} + u^2 + \frac{3}{4}u^{5/2} + \frac{10}{3}u^3 + \frac{1487}{320}u^{7/2} - \frac{1}{3}u^4 + \cdots \tag{4.6}$$

The first two terms of this expansion may be derived via a simple entropy of mixing argument applied to a collection of noninteracting vacancies. The higher-order terms include effects of the vacancy pair potential, U_c. Since Eq. (4.6) was derived from the low temperature expansion for $\kappa_a(T)$, we expect it to be valid for the compact animal regime, $y > y_c$, where y_c is the y value corresponding to $\bar{\varepsilon}(T_c)$. Employing the estimate $T_c = 0.54$ in Eq. (4.2) yields $\bar{\varepsilon}(T_c) = -1.87$, so that $y_c \simeq 0.87$.

In Fig. 6 we plot the asymptotic scaling function $g(y)$. For $y \leqslant 0.65$, g is estimated from the $\sigma_{p,k}$ data (broken line). The other branch (solid line) is given by Eq. (4.6), using the Sykes–Glen estimate[11] $\sigma = 1.401$. We propose the following interpretation of Fig. 6. The small-y branch (broken line) represents a portion of the scaling function for noncompact or

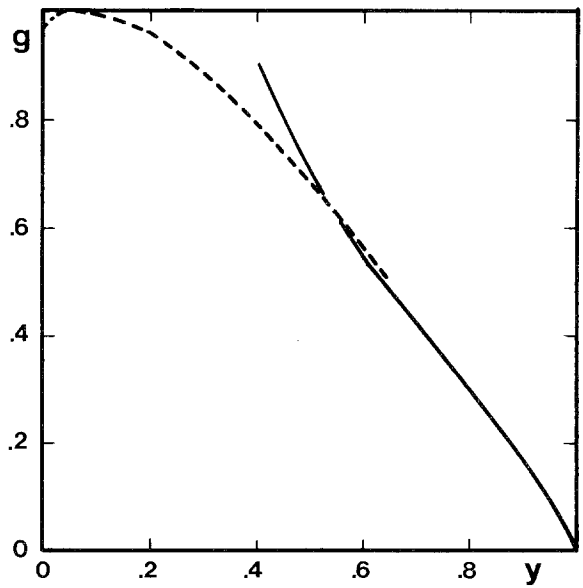

Fig. 6. Asymptotic scaling function, $g(y)$, versus y. Solid line: Eq. (4.6) with $\sigma = 1.401$. Broken line: extrapolation from finite-p data.

ramified animals, while Eq. (4.6) describes the compact regime. We expect the two branches to join smoothly at y_c. The meeting point marks the collapse transition, and since this transition is second order,[6] we expect d^2g/dy^2 to vanish at this point.[18] Our interpretation is supported by the fact that the two branches of $g(y)$, computed by different methods, are nearly in agreement for $y \simeq 0.6$. However, numerical data for larger animals ($p > 100$) will be required in order to determine $g(y)$ in the neighborhood of y_c. A systematic *high-temperature* expansion, as well as additional terms in the low-temperature expansion for $\kappa_a(T)$, would also be valuable for understanding critical and scaling behavior.

APPENDIX A: BOUND ON THE ENERGY ERROR IN Z'_p

Let $X = \{x_1, ..., x_p\} \subset \mathbf{Z}^2$ be an animal configuration, with perimeter $\Gamma(X)$ and perimeter length $B(X)$. (We assume that $p = n^2$, n an integer.) $\Gamma(X)$ encloses p occupied and v_{in} vacant sites. For $x \in X$, define the valence $v(x)$ as the number of occupied nearest neighbors of x. The total number of nearest-neighbor bonds in X is

$$k(X) = \frac{1}{2} \sum_{x \in X} v(x) \tag{A.1}$$

Suppose that all $p + v_{in}$ sites within $\Gamma(X)$ were occupied. Then, since there are exactly $B(X)$ lattice bonds from sites within $\Gamma(X)$ to sites outside $\Gamma(X)$, the sum of the valences of the sites within $\Gamma(X)$ would be $4(p + v_{in}) - B(X)$. If the sites $\bar{x}_1, ..., \bar{x}_{v_{in}}$, enclosed by $\Gamma(X)$, are now vacated, a total of $4v_{in} + U(\bar{x}_1, ..., \bar{x}_{v_{in}})$ bonds are lost. The number of nearest-neighbor bonds in X is therefore given by Eq. (2.6).

Now suppose that $X \subset \Lambda_{p+v}$, a square of side $\sqrt{p} + m$. The total number of vacant sites in Λ_{p+v}, $v = v_{in} + v_{out}$, is the cardinality of $\bar{X} \equiv \Lambda_{p+v} \backslash X$. Let $\bar{X}_{in}$ and $\bar{X}_{out}$ denote, respectively, the portions of $\bar{X}$ lying within and outside of $\Gamma(X)$. By construction, if $\bar{x} \in \bar{X}_{in}$ and $\bar{x}' \in \bar{X}_{out}$, then $\bar{x}$ and $\bar{x}'$ cannot be nearest neighbors, and so $U(\bar{X}) = U(\bar{X}_{in}) + U(\bar{X}_{out}) \equiv U_{in} + U_{out}$. Thus

$$\Delta E \equiv -2(p - v) + U(\bar{X}) + k(X) = 2v_{out} + U_{out} - \tfrac{1}{2}B(X) \tag{A.2}$$

For $\bar{x} \in \bar{X}_{out}$, let $v(\bar{x})$ be the number of sites in $\bar{X}_{out}$ which are nearest neighbors of $\bar{x}$. Then since $-U_{out}$ is the number of nearest-neighbor pairs within $\bar{X}_{out}$

$$U_{out} = -\tfrac{1}{2} \sum_{\bar{x} \in \bar{X}_{out}} v(\bar{x}) = -2v_{out} + \tfrac{1}{2}B(\bar{X}_{out}) \tag{A.3}$$

where $B(\bar{X}_{out})$ is the sum of the lengths of the perimeters separating $\bar{X}_{out}$ from X *and* from $\mathbf{Z}^2 \backslash \Lambda_{p+v}$. ($\bar{X}_{out}$ may consist of several components which

are not connected.) We may write the total perimeter length of $\bar{X}_{\text{out}}$ as $B(\bar{X}_{\text{out}}) = v_e + 2v_c + B_i$, where v_e and v_c are, respectively, the number of vacancies lying at edges and coners of Λ_{p+v}, and B_i is the length of the portion of $\Gamma(X)$ which lies within Λ_{p+v}, i.e., the length of $\Gamma(X)\backslash[\Gamma(X) \cap \Gamma(\Lambda_{p+v})]$ (see Fig. 7). Thus $B_i = B(X) - p_e - 2p_c$, where p_e and p_c are, respectively, the number of occupied sites at edges and corners of Λ_{p+v}. Since Λ_{p+v} is a square of side $\sqrt{p}+m$, $p_e + v_e = 4[\sqrt{p}+m-2]$, and noting that $p_c = 4 - v_c$, we have $B(X) - B_i = 4(\sqrt{p}+m) - v_e - 2v_c$. Thus

$$U_{\text{out}} = -2v_{\text{out}} + \tfrac{1}{2}B(X) - 2(\sqrt{p}+m) + v_e + 2v_c \tag{A.4}$$

Combined with Eq. (A.2), this yields Eq. (2.7).

APPENDIX B. LOW-TEMPERATURE EXPANSION FOR $\kappa_c(T)$

We apply the Ursell expansion to the evaluation of

$$\kappa_c(T,\mu) = \lim_{N\to\infty} N^{-1} \log\left[\xi^{2N}\lambda^{-N} \sum_{n=0}^{1} \frac{\xi^{-4Nn}\lambda^{Nn}}{(Nn)!} \times \sum_{x_1,\ldots,x_{Nn}\in\Lambda_N} e^{-U_c(x_1,\ldots,x_{Nn})/T}\right] \tag{B.1}$$

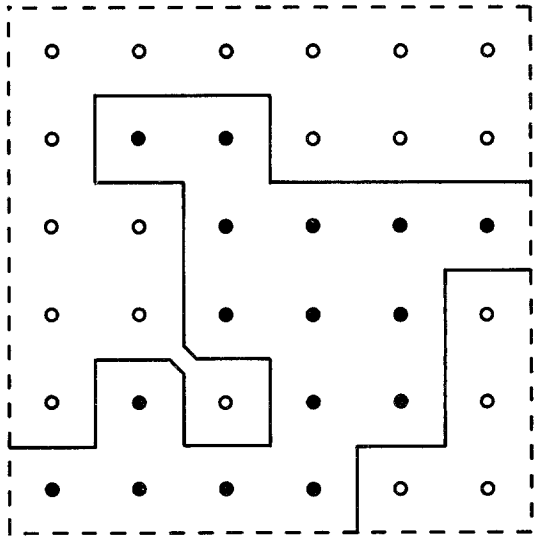

Fig. 7. An animal configuration X (filled circles) contained within a square, Λ_{p+v}. The perimeter of Λ_{p+v} is indicated by the broken line, and the perimeter of X within Λ_{p+v} is indicated by the solid line. For this configuration, $p = 16$, $k = 18$, $B = 28$, $v = v_{\text{out}} = 20$, $v_e = 12$, $v_c = 3$, and $U_{\text{out}} = -20$.

Our treatment follows the approach of Ref. 22. Let

$$\Xi_{\Phi}(N, T, z) = \sum_{m=0}^{N} \frac{z^m}{m!} \sum_{x_1,\ldots,x_m \in \Lambda_N} e^{-\Phi(x_1,\ldots,x_m)/T} \tag{B.2}$$

be the grand partition function for a lattice gas of N sites, at temperature T and fugacity z. The potential, Φ, may include many-body interactions. The Ursell expansion for the free energy density is

$$\lim_{N\to\infty} N^{-1} \log \Xi_{\Phi}(N, T, z) = \sum_{r=1}^{\infty} b_r(T)\, z^r \tag{B.3}$$

where

$$b_r(T) = \frac{1}{r!} \sum_{x_1 = 0; x_2,\ldots,x_r \in Z^2} u(x_1,\ldots, x_r) \tag{B.4}$$

(We assume that the potential Φ is such that the limit in Eq. (B.3) exists. For the potentials U and U_c this poses no problem). To define $u(x_1,\ldots, x_r)$ we introduce

$$\begin{aligned} w(x_1) &\equiv w_1 = 1 \\ w(x_1, x_2) &\equiv w_{12} = e^{-\Phi(x_1, x_2)/T} \\ w(x_1, x_2, x_3) &\equiv w_{123} = e^{-\Phi(x_1, x_2, x_3)/T} \end{aligned} \tag{B.5}$$

etc. Then $u(x_1,\ldots, x_r)$ is the sum over all possible products of w's, such that the subscripts on the w's run through $\{1,\ldots, r\}$ with each index occurring exactly once. A product of k factors has the coefficient $(-1)^{k-1}(k-1)!$ Thus

$$\begin{aligned} u(x_1, x_2) &= w_{12} - w_1 w_2 = w_{12} - 1 \\ u(x_1, x_2, x_3) &= w_{123} - w_{12} - w_{23} - w_{13} + 2 \end{aligned} \tag{B.6}$$

etc. We note that if $X = \{x_1,\ldots, x_r\}$ can be divided into subsets X_1 and X_2 such that $\Phi(X) = \Phi(X_1) + \Phi(X_2)$, then $u(x_1,\ldots, x_r) = 0$. We call such configurations "Φ-disconnected."

Comparing Eqs. (B.1) and (B.2), we see that Eq. (2.16) holds if we let $g_r^c = \eta^{2r} b_r^c$, where b_r^c is given by Eq. (B.4) with $\Phi = U_c$. (If we let $\Phi = U$ we obtain Eq. (2.11), where $g_r = \eta^{2r} b_r$.) Since U and U_c are identical for configurations of three of fewer vacancies, $g_r^c = g_r$ for $r \leqslant 3$. In evaluating the sum over configurations in Eq. (B.4), it is helpful to introduce a graphical

notation. We represent each vacancy by a dot, join dots representing nearest-neighbor pairs by a straight line (•——•), and join dots representing vacancies occupying the same site by a wavy line (•〰〰•). We denote a quartet of vacancies encircling an occupied site by

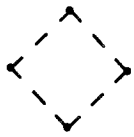

Each U_c-connected r-point graph makes a contribution to b_r which is a product of: (1) a labeling factor—the number of distinct ways of assigning the labels 1,..., r to the points; (2) an embedding factor—the number of translationally nonequivalent arrangements in the lattice which realize the bonding structure; and (3) $u(x_1,..., x_r)$. To compute $g_r^c - g_r$ we identify the r-point graphs which involve a many-body term in $U_c - U$, and evaluate the factors listed above. For $r=4$, the only graph is the one depicted above, and its contribution to $g_4^c - g_4$ is $-\eta^8$. For $r=5$ the graphs and their contributions are listed below:

Graph	Contribution $g_5^c - g_5$
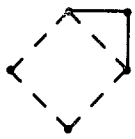	$-4\eta^8 + 4\eta^{10}$
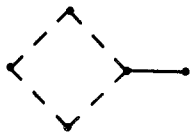	$-4\eta^9 + 4\eta^{10}$
	$8\eta^{10}$
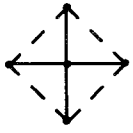	η^{10}

(Note that in the configuration

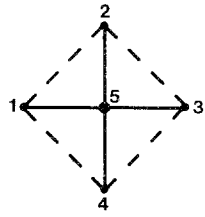

$U_c(x_1, x_2, x_3, x_4) = +\infty$, but $U_c(x_1, x_2, x_3, x_4, x_5) = -4$. The full configuration does not violate connectivity.) Hence $g_5^c - g_5 = -4\eta^8 - 4\eta^9 + \eta^{10}$. The remaining terms in Eq. (2.17) are obtained in the same manner.

APPENDIX C. ASYMPTOTIC SCALING FORMULA

Let $\sigma_{p,k}^L$ be the number of translationally nonequivalent p-particle, k-bond animals in lattice L. In Ref. 18 we showed that for $p-1 \leqslant k \leqslant k_m(p)$ (and for k' and p' similarly related),

$$\sigma_{p+p',k+k'+1}^L \geqslant \sigma_{p,k}^L \sigma_{p',k'}^L \tag{C.1}$$

In Ref. 21 we showed that if L is the square, triangle, hexagon, simple cubic, body- or face-centered cubic lattice, then there is a finite constant $c(L)$ such that $\sigma_{p,k}^L < e^{c(L)p}$. According to a result in the theory of subadditive functions,[23] if Y_p ($p = 1, 2, 3, \ldots$) is a sequence with $Y_1 > 0$, and $Y_{p+p'} \geqslant Y_p Y_{p'}$, and if $y_p \equiv p^{-1} \log Y_p < c < \infty$, then $\lim_{p \to \infty} y_p$ exists.

Let r and s be positive integers such that $q/2 > s/r \geqslant 1$ (q is the coordination number of the lattice). Then the results cited above imply that

$$\lim_{n \to \infty} n^{-1} \log \sigma_{nr,ns-1}^L \equiv r\tilde{g}_L\left(\frac{s}{r}\right) \tag{C.2}$$

exists. Thus as $n \to \infty$

$$\log \sigma_{nr,ns-1}^L \sim nr\tilde{g}_L\left(\frac{s}{r}\right) + o(n) \tag{C.3}$$

We may recast Eq. (C.1) in the form

$$\sigma_{nr,ns-1}^L \geqslant \sigma_{nt,nu-1}^L \sigma_{n(r-t),n(s-u)-1}^L \tag{C.4}$$

If we take the logarithm, divide by nr, and use Eq. (C.3), then in the limit $n \to \infty$ we obtain

$$\tilde{g}_L\left(\frac{s}{r}\right) \geqslant \frac{t}{r}\tilde{g}_L\left(\frac{u}{t}\right) + \frac{r-t}{r}\tilde{g}_L\left(\frac{s-u}{r-t}\right) \tag{C.5}$$

If we now let $x = u/t$, $y = (s-u)/(r-t)$, and $a = t/r$, we find

$$\tilde{g}_L[ax + (1-a)\, y] \geqslant a\tilde{g}_L(x) + (1-a)\, \tilde{g}_L(y) \tag{C.6}$$

for x, y, and a rational, $x, y \in [1, q/2)$, and $|a| < 1$. Thus $\tilde{g}_L$ is concave, hence continuous, on the rationals in $[1, q/2)$. Letting $nr = p$, $ns - 1 = k$, and using the continuity of $\tilde{g}_L$, we may rewrite Eq. (C.3) as

$$\log \sigma_{p,k}^{L} \sim p\tilde{g}_L\left(\frac{k}{p}\right) + o(p) \qquad (p \to \infty) \tag{C.7}$$

which is the desired scaling formula. $\tilde{g}_L$ may be extended to $[1, q/2]$ by continuity, but for the study of animal statistics, its restriction to the rationals in this interval is sufficient.

ACKNOWLEDGMENT

We thank Professor S. G. Whittington for drawing our attention to Ref. 10. One of us (R.D.) acknowledges partial support by the Robert A. Welch Foundation.

REFERENCES

1. O. Penrose and J. L. Lebowitz, in *Fluctuation Phenomena*, E. W. Montrol and J. L. Lebowitz, eds. (North-Holland, Amsterdam, 1979).
2. C. Domb, *J. Phys. A* **9**:283 (1976).
3. K. Binder, *Ann. Phys. (N.Y.)* **98**:390 (1976).
4. D. Stauffer, *Phys. Rep.* **54**:1 (1979).
5. J. W. Essam, *Rep. Prog. Phys.* **43**:53 (1980).
6. B. Derrida and H. J. Herrmann, *J. Phys.* **44**:1365 (1983).
7. R. Dickman and W. C. Schieve, *J. Phys.* **45**:1727 (1984).
8. H. E. Stanley, P. J. Reynolds, S. Redner, and F. Family, in *Real-Space Renormalization*, T. W. Burkhardt and J. M. J. van Leeuwen, eds. (Springer-Verlag, Berlin, 1982).
9. S. Havlin, Z. V. Djordjevic, I. Majid, H. E. Stanley, and G. W. Weiss, *Phys. Rev. Lett.* **53**:178 (1984).
10. S. G. Whittington, G. M. Torrie, and D. S. Gaunt, *J. Phys. A* **16**:1695 (1983).
11. M. F. Sykes and M. Glen, *J. Phys. A* **9**:87 (1976); M. F. Sykes, D. S. Gaunt, and M. Glen, *J. Phys. A* **9**:1705 (1976).
12. A. B. Harris and T. C. Lubensky, *Phys. Rev. B* **23**:3591 (1981).
13. B. Derrida and L. DeSeze, *J. Phys.* **43**:475 (1982).
14. P. L. Leath and G. R. Reich, *J. Phys. C* **11**:4017 (1978).
15. D. Stauffer, *Phys. Rev. Lett.* **41**:1333 (1978).
16. H. P. Peters, D. Stauffer, H. P. Holters, and K. Loewenich, *Z. Phys. B* **34**:399 (1979).
17. G. Jacucci, A. Perini, and G. Martin, *J. Phys. A* **16**:369 (1983).
18. R. Dickmann and W. C. Schieve, *J. Stat. Phys.* **33**:527 (1983).

19. M. F. Sykes, J. W. Essam, and D. S. Gaunt, *J. Math. Phys.* **6**:283 (1965); M. F. Sykes, D. S. Gaunt, J. W. Essam, C. J. Elliott, and S. R. Mattingly, *J. Math. Phys.* **14**:1066 (1973); M. F. Sykes, D. S. Gaunt, J. W, Essam, B. R. Heap, C. J. Elliott, and S. R. Mattingly, *J. Phys. A* **6**:1498 (1973).
20. C. Domb, in *Phase Transitions and Critical Phenomena*, C. Domb and M. S. Green, eds. (Academic Press, New York, 1974), Vol. 3, p. 357.
21. R. Dickman and W. C. Schieve, *J. Stat. Phys.* **36**:435 (1984).
22. C. Domb, in *Phase Transitions and Critical Phenomena*, C. Domb and M. S. Green, eds. (Academic Press, New York, 1974), Vol. 3, p. 1.
23. E. Hille, *Functional Analysis and Semigroups* (American Mathematical Society, New York, 1948), Theorem 6.6.1.